J Mater Sci (2011) 46:6772–6782
DOI 10.1007/s10853-011-5634-1

Photo-immobilized heparin micropatterns on Ti–O surface: preparation, characterization, and evaluation in vitro

Lijuan Lei · Chunhui Li · Ping Yang · Nan Huang

Received: 14 March 2011 / Accepted: 12 May 2011 / Published online: 1 June 2011

Abstract In order to harmonize the functions of both anticoagulation and accelerating endothelialization simultaneously, the micropatterns were fabricated by photoimmobilizing heparin, functionalized with a photoreactive moiety, on 3-aminopropylphosphonic acid modified titanium oxide (Ti–O) substrates. The amount of heparin immobilized on the surfaces was determined using the toluidine blue assay. And the surface morphology of the patterns was examined using scanning electron microscopy and surface profiler. The platelet adhesion and endothelial cell behavior in terms of adhesion, proliferation, and orientation were investigated in vitro. It is clear that the heparin patterns can reduce the platelet adhesion, and promote endothelial cells spreading and proliferation compared to nonpatterned heparin sample. Furthermore, the microstripes with appropriate size can induce the cells to elongate and arrange along the stripe direction. This may suggest a new modification method for blood-contacting device.

Introduction

Hemocompatibility is regarded as a key property for blood-contacting devices. Among the methods of improving hemocompatibility, immobilizing anticoagulant biomolecules and endothelialization are widely used [1–3]. The biomaterials covered with a layer of endothelial cells can achieve the desired biolization, decreasing the incidence of thrombosis and indicating good biocompatibility [2, 3]. However, a surface with anticoagulant biomolecules, such as heparin [1, 4] and human serum albumin [5, 6], can effectively inhibit the thrombus formation or platelet adhesion [5, 7, 8] but usually resist to endothelial cell adhesion [9, 10], which is always used for the short-term antithrombotic demand [11]. Meanwhile, the surface covered with biomolecules that can promote endothelialization also induces platelets adhesion [12, 13] and thrombosis [14]. Therefore, it is quite valuable for the cardiovascular implants to fabricate a surface which can harmonize the functions of both anticoagulation and accelerating endothelialization simultaneously by coating two different chemical components, one inhibits platelet adhesion and the other promotes endothelialization. Micropatterning [15–18], as a feasible method to enable visualization of the effect of surface properties on cell functions such as proliferation, differentiation, and apoptosis [19], provides an opportunity to pattern the substrate with two distinctly different regions in terms of chemistry [20]. Furthermore, the cell alignment, dictating their biological and mechanical function [21], is also modulated by micropatterns [22].

Heparin, as an anticoagulation biomolecule, can enhance antithrombin III affinity with thrombin [23], accelerate inactivation of thrombin [24], and inhibit platelet adhesion and aggregation [25]. It has been widely used to modify the surface of blood contact materials due to its good antithrombin property [26]. Titanium oxide (Ti–O) thin films were used as the basis because of its good biocompatibility and bioinertness [27]. Alkanephosphonic acid can form a self-assembled monolayer (SAMs) on Ti–O surface [28, 29], and provide a bridge for heparin photo-immobilization. In addition, the SAMs terminated with amine group is beneficial for cell adhesion, spreading,

L. Lei · C. Li · P. Yang (✉) · N. Huang
Key Laboratory of Advanced Materials Technology of Education Ministry, Key Laboratory of Artificial Organ Surface Engineering of Sichuan, School of Materials Science and Engineering, Southwest Jiaotong University, Chengdu 610031, People's Republic of China
e-mail: yangping8@263.net

and growth [30, 31]. The aim of this research is to prepare the micropatterns of heparin and amine-terminated alkanephosphonic acid on Ti–O films to harmonize their benefits to both anticoagulation and endothelialization and to study their influence on platelet adhesion and endothelial cell behavior. In this study, the patterns were prepared as follows: First, azido group was introduced into heparin molecules to act as a photoreactive point. Second, Ti–O films were modified by amine-terminated alkanephosphonic acid with functional group for covalently immobilizing heparin. Finally, heparin was immobilized via UV irradiation in the present of mask and a surface with heparin patterns was fabricated. The blood and cell compatibilities were evaluated by platelet adhesion and endothelial cells culture.

Experimental details

Preparation of Ti–O films

The Ti–O films were prepared on silicon (100) wafers by unbalanced magnetron sputtering system using a titanium target (purity 99.99%) in the mixed Ar/O_2 atmosphere. Before sputtering, the silicon substrate and the titanium target were pre-sputtered in an argon atmosphere in order to remove the impurity on the silicon surface and surface layer on the metallic titanium target for approximately 6 and 3 min, respectively. Afterward, argon and oxygen were independently introduced into the chamber as sputtering and working gas, respectively. The deposition time was 15 min. The details of sputtering conditions are listed in Table 1.

Synthesis of photoreactive heparin

Photoreactive heparin was synthesized as follows: 200 mg of heparin sodium (Santa Cruz Biotechnology, China) was dissolved in 200 mL distilled water with 40 mg of 4-azidoaniline and the mixture of 69.05 mg of *N*-hydroxysuccinimide (NHS, Sigma-Aldrich), 191.7 mg of *N*-(3-dimethylaminopropyl)-*N*′-ethylcarbodiimide (EDC, Sigma-Aldrich), and 2333.7 g of 2-morpholinoethane sulfonic acid (MES, Sigma-Aldrich). The solution was stirred at 4 °C for 24 h in dark and its pH was adjusted to 7.0 with 0.1 M NaOH. Then the solution was dialyzed using a cellulose ester dialysis membrane (cut off MW 8,000) and the residue was repeatedly washed with distilled water until the absence of 4-azidoaniline in the filtrate was confirmed by ultraviolet absorption. The purified solution was then lyophilized and the photoreactive heparin conjugate was obtained and referred to as AzHep. The synthetic scheme of photoreactive heparin is shown in Fig. 1. Heparin is a heterogeneous mixture of sulfated polysaccharides with repeating sugar unites, and each unit include two carboxyl groups which can form amide bond with amino group of 4-azidoaniline. There will be three kinds of distribution of the azidophenyl group in the heparin molecule.

The presence of the azidophenyl groups in the heparin was determined by ultraviolet absorbance spectra (UV-2550, Shimadzu, Japan) and Fourier transform infrared spectroscopy (FTIR, Nicolet 5700, USA). Ultraviolet absorbance spectra of original heparin, 4-azidoaniline, and AzHep solution were used to detect the maximum absorption in the range of 200–600 nm. Transmission spectrum of original heparin and AzHep were tested by FTIR, and 32 scans spectra were collected in the range of 100–4000 cm^{-1}, and gold was used as the background spectra for analysis purposes.

Table 1 Synthesis parameters of Ti–O films

Experimental parameters	Values
Oxygen flow (sccm)	13
Argon flow (ccm)	60
Base vacuum ($\times 10^{-3}$ Pa)	<2.0
Base bias voltage (V)	0
Sputtering voltage (V)	340–375
Sputtering current (A)	3
Substrate temperature (°C)	72–159
Deposition pressure (Pa)	0.63
Substrate-to-target distance (mm)	100
Deposition time (min)	15

Phosphonated treatment of Ti–O

In order to optimize the hydrophilic properties, the Ti–O substrates were cleaned in piranha solution (3:1 v/v 98% H_2SO_4/30% H_2O_2) for 30 min. After rinsed with distilled water and blown dry at room temperature, Ti–O substrates were placed into a 10 mM aqueous solution of 3-aminoprophylphosphonic acid (APPA, Sigma-Aldrich) at 80 °C for 4 h. Then the functionalized substrates were washed with distilled water to remove physically absorbed APPA, and referred to as APPA/Ti–O.

APPA/Ti–O was characterized by FTIR with a FT80 grazing angle infared reflection accessory. The spectrum was recorded under nitrogen to eliminate the background signal due to CO_2 and H_2O absorption bands, and the unmodified Ti–O substrates were used as the background spectra for analysis purposes. Typically, 1024 scans were collected for APPA/Ti–O in the range of 100–4000 cm^{-1}. The surface elemental compositions were measured by X-ray photoelectron spectroscopy (XPS, XSAM800, Kratos Ltd, UK) with a monochromatic Mg Kα (1253.6 eV) X-ray source at 12 kV and a pressure of $5–7\times 10^{-9}$ mbar.

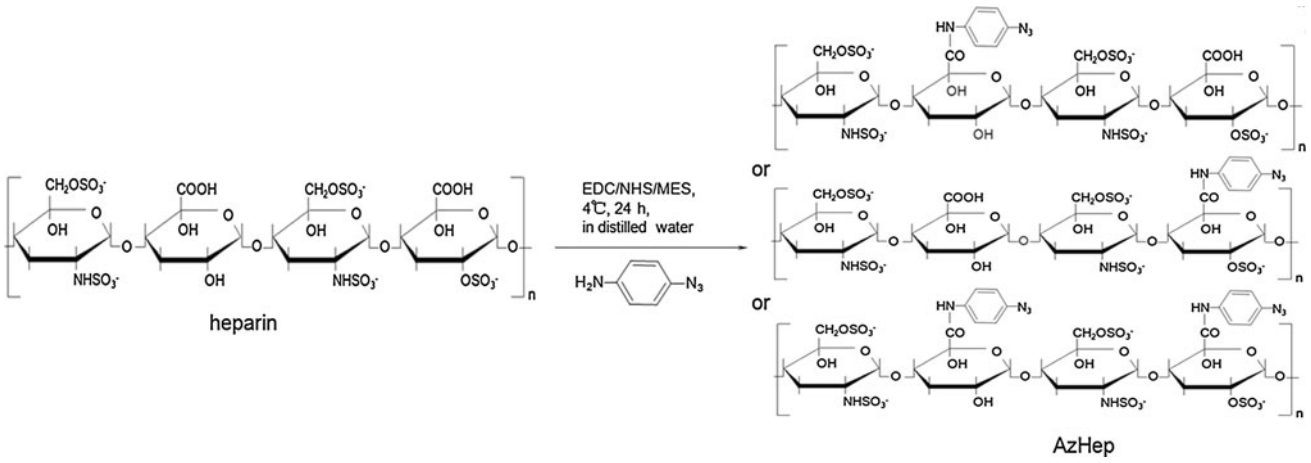

Fig. 1 The synthetic scheme of photoreactive heparin

The static water contact angles (CA, sessile drop method) were detected using a contact angle apparatus (JY-82, China) at room temperature. For each sample, the mean value was obtained from five individual measurements taken at different spots where 10 μL of deionized water were dropped on. Five samples were measured in order to obtain statistical results for one type of surface.

Photo-immobilization of photoreactive heparin

Upon UV irradiation, the azidophenyl group of AzHep eliminated N_2 and generated nitrene, a highly reactive intermediate that has a property of binding to a C–H bond or N–H bond through insertion reaction [32, 33]. Thus, the photoreactive heparin could cross-link with APPA and heparin molecules. The microprocessing procedure is shown in Fig. 2. An aqueous solution of AzHep (0.1 mL, 40 mg/mL) was dropped on the APPA/Ti–O substrate, spin-coated, and air-dried at room temperature in dark. Subsequently, the samples were irradiated with an UV lamp (365 nm, 8.5 mW/cm^2) at a distance of 10 cm for 300 s in the presence of a chromium–quartz photomask with a grating pattern. After irradiation, the samples were rinsed with distilled water three times to dissolve the unirradiation AzHep. Finally, alternating planar-chemical stripes of heparin and APPA were prepared on Ti–O substrate. The width of the heparin was decided by the width of the grating crack (25, 14, and 10 μm). So the patterned heparin samples were labeled as Pa/b, expressing the width of parallel heparin and APPA modified Ti–O stripes, respectively (shown in Fig. 2). Here four different stripes were prepared and denoted as P25/25, P25/15, P14/7, and P10/5, respectively. The immobilized heparin sample prepared without the photomask was labeled as HEP.

The static water contact angle of HEP was detected at room temperature. The amount of heparin immobilized on the surfaces was determined using the toluidine blue assay as previous report [34].The surface morphology of the patterned samples was examined using a scanning electron microscopy (SEM, Philips, The Netherlands). The profile of patterns was measured using high-resolution surface profiler (XP-2, Ambios Technology Inc., USA).

Platelets adhesion

The whole blood of a healthy adult volunteer was immediately centrifuged for 15 min at 1500 rpm to obtain platelet-rich plasma (PRP). The samples were cut into

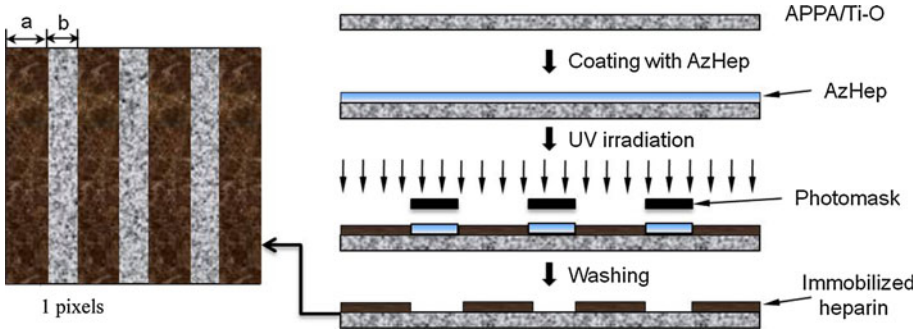

Fig. 2 Micropattern-immobilization of AzHep on APPA/Ti–O surface by UV irradiation

squares of 7 × 7 mm^2, and three parallel samples in each group were prepared. After being placed in the 24-well culture plate and incubated with 0.5 mL of PRP for 2 h at 37 °C, the samples were rinsed with phosphate buffered solution (PBS) to remove the nonadherent platelets. Subsequently, the adhered platelets were fixed in 2.5% glutaraldehyde solutions, and then dehydrated, dealcoholized, and dried in a CO_2 critical point drier (CPD030, Balzers) for SEM observation. Ten different field of 280 × 212 μm^2 for each sample were randomly chosen to obtain good statistical results of the number of adhered platelets by optical microscopy [35, 36].

Endothelial cell culture

Endothelial cells were isolated according to the method described by Chen et al. [37]. The endothelial cells were incubated in M199 medium supplemented with 20% (v/v) fetal bovine serum (Hyclone), 15 U/mL heparin, and 20 μg/mL endothelial cell growth supplement (ECGS, Sigma) at 37 °C in 5% CO_2 incubator. The first passage of endothelial cells with the concentration of 5 × 10^4 cells/mL were seeded on the sterilized samples and incubated at 37 °C for 4 h, 1 day, and 3 days, respectively. At the predetermined time points, the samples were washed with PBS for three times, fixed with 2.5% glutaraldehyde solutions at room temperature. The fixed samples were rinsed three times with PBS for 15 min each, and then dehydrated, dealcoholized, followed by drying for optical microscopy examination.

The number of attached cells was assayed by CCK-8 (Cell Counting Kit-8, Dojindo, Japan) [38]. 400 μL M199 medium with 40 μL CCK-8 was added to each pre-cultured sample and then the samples were incubated in 5% CO_2 incubator for 3 h at 37 °C. The absorbance at 450 nm was determined using a microplate reader.

The statistical analysis about the overall cell area, length, breadth, and orientation angle α of cells were measured by UTHSCSA Image Tool 2.0 according to the methods reported [39], as shown in Fig. 3. Measurements were made on cells in five random optical microscope fields of 700 × 530 μm^2 for each sample. Length/breadth (L/B) was used to define the cell elongation index [40], and the cells whose cellular orientation angle was within 10° were considered to be aligned [22].

Statistical analysis

All data were presented as the mean ± standard deviation (SD). The statistical significance between the groups was assessed using the SPSS11.5 software. The probability value $p < 0.05$ was considered to be of significant difference.

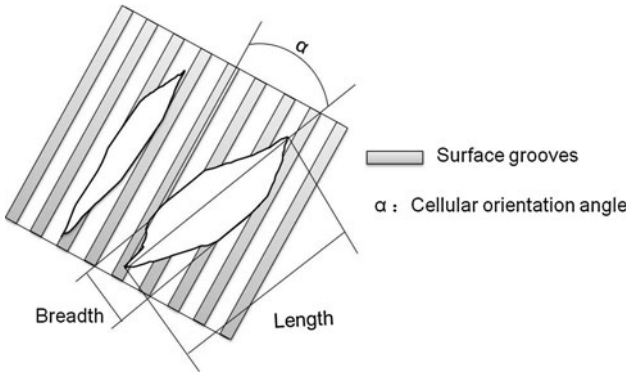

Fig. 3 Digital image analysis parameters: Length, breadth, and cellular orientation angle

Results and discussion

Synthesis of photoreactive heparin

Ultraviolet and FTIR spectra of original heparin and AzHep are shown in Figs. 4 and 5, respectively. In the ultraviolet spectrum of AzHep, an absorption at 269 nm assigned to azidophenyl group was observed. And it was somewhat red-shifted from the corresponding absorption of 4-azidoaniline, which could be ascribed to electron delocalization of azidophenyl group caused by the amide bond formation [41]. Compared to original heparin, the FTIR spectrum of AzHep showed a strong stretching vibration of $C–N_3$ at 2130 cm^{-1}. The results above confirm that the azide group has been introduced into heparin molecule.

APPA modified Ti–O

It has been reported that alkanephosphonic acid could form SAMs on native or anatase Ti–O surface [28, 29]. In

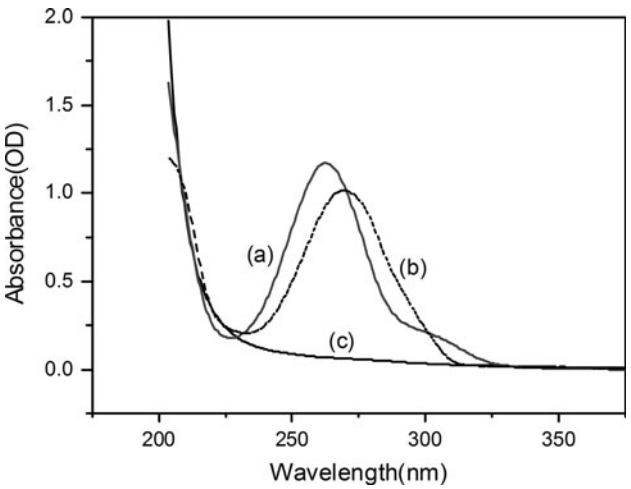

Fig. 4 Ultraviolet absorbance spectra of (*a*) 4-azidoaniline (15 μg/mL), (*b*) AzHep (100 μg/mL), and (*c*) original heparin (1 mg/mL)

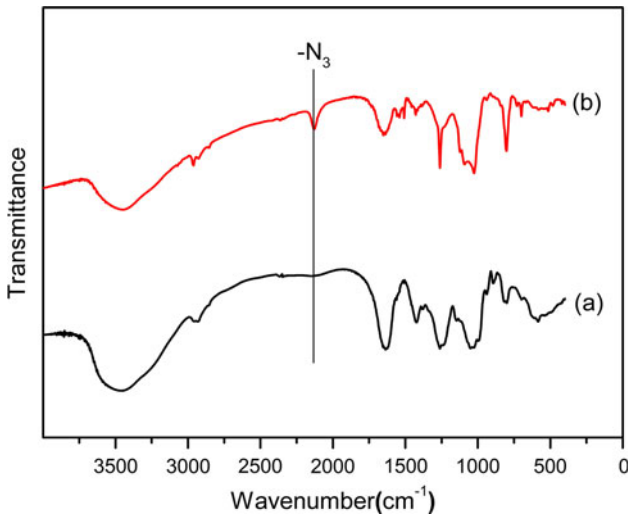

Fig. 5 FTIR spectra of (*a*) original heparin and (*b*) AzHep

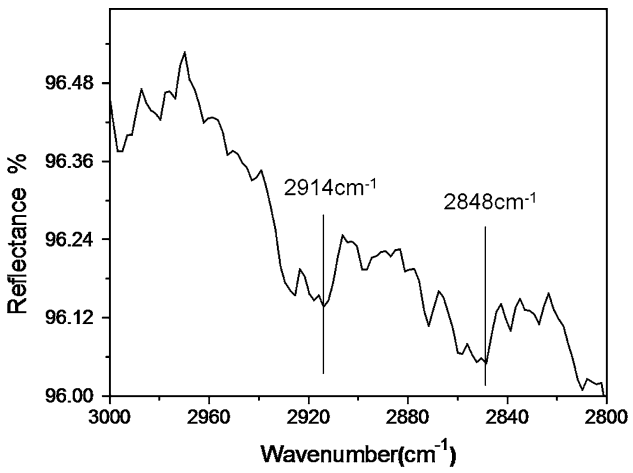

Fig. 6 FTIR spectrum of APPA/Ti–O surface

general, the C–H stretches of the methylene group are used as the reference peaks for SAMs organization on substrates [42]. The C–H stretch has two common vibrations: a symmetric stretch and an asymmetric stretch corresponding to a peak at ~2850 and ~2918 cm^{-1}, respectively [43]. In Fig. 6, two very weak peaks at 2914 and 2848 cm^{-1} can be found in FTIR spectrum of APPA/Ti–O. The XPS and contact angle analysis were used to further confirm the assembly of APPA on Ti–O surface. The surface elemental composition based on XPS full survey spectra are listed in Table 2. The surface composition of Ti–O became different after treatment with APPA, and the increase of P and N could be attributed to APPA assembled on surface. Consistent with the XPS results, a remarkable decrease of the water contact angle from 69° to 34° after APPA treatment indicated the hydrophilicity improvement of Ti–O surface caused by the APPA coverage.

Table 2 The surface elemental composition obtained by XPS analysis

Sample	P (%)	N (%)	TI (%)	O (%)	C (%)
Ti–O	0	0.37	6.24	14.06	79.33
APPA/Ti–O	1.26	1.10	6.16	12.66	78.83

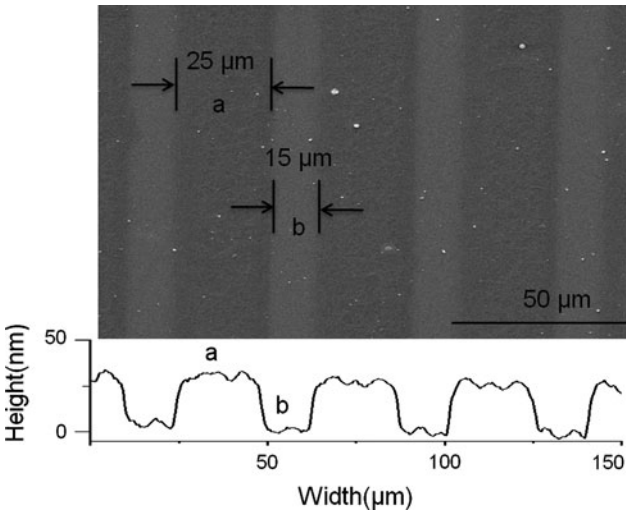

Fig. 7 Micrograph and profile of sample P25/15: alternating stripes of (*a*) heparin and (*b*) APPA modified Ti–O

Photo-immobilization of AzHep

Upon UV irradiation, the photoreactive heparin could be covalently immobilized on APPA/Ti–O surface. The water contact angle of HEP was 59°, indicating a remarkable increase compared to APPA/Ti–O. Because carboxyl groups of heparin was consumed and phenyl group was brought when the photoreactive group was introduced into heparin molecule. The results of toluidine blue assay revealed that the amount of heparin immobilized on HEP was 3.8 ± 0.7 μg/cm^2, indicating the successful immobilization of heparin on the surface. Figure 7 displays the surface micrograph and profile of patterned sample (P25/15). The pattern consisted of alternative heparin and APPA modified Ti–O stripes. The width of heparin and APPA modified Ti–O stripes were 25 and 15 μm, respectively. The height of the heparin stripe was about 30 nm.

Interaction with platelets

The adhesion and activation of platelets on materials surface are considered as an early indicator of thrombogenicity of blood-contacting device [44]. When a foreign material contacts blood, plasma proteins adsorb to the surface, followed by the platelet adhesion, then the adherent platelets become activated, secrete agonists that

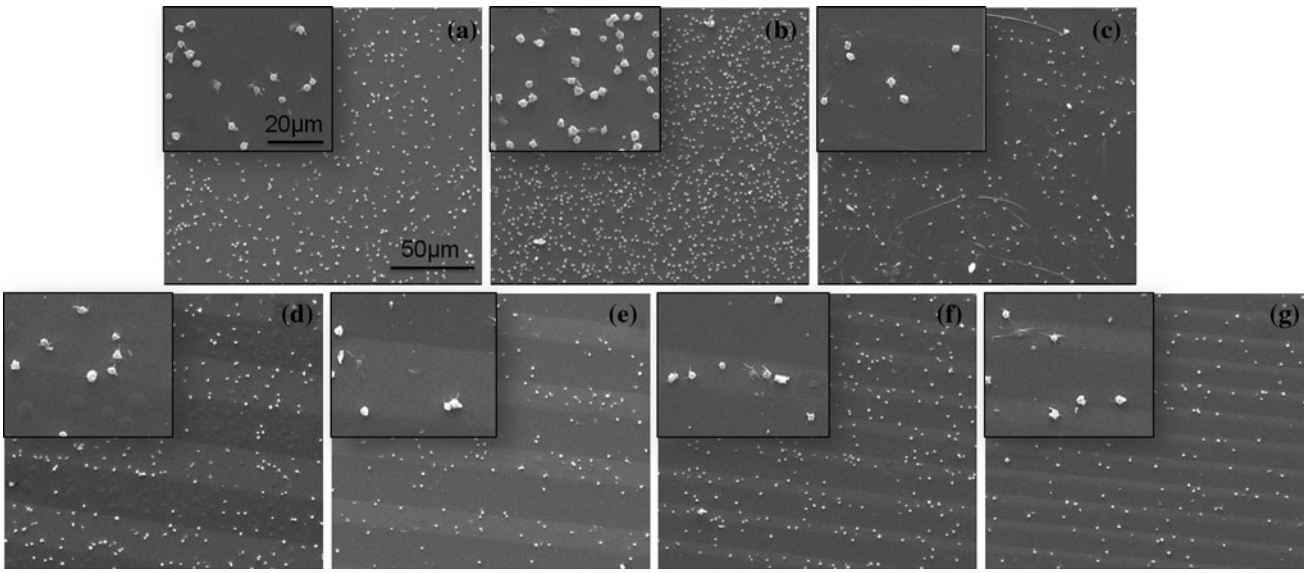

Fig. 8 SEM images of platelets adhesion on the surfaces of **a** Ti–O, **b** APPA/Ti–O, **c** HEP, **d** P25/25, **e** P25/15, **f** P14/7, and **g** P10/5

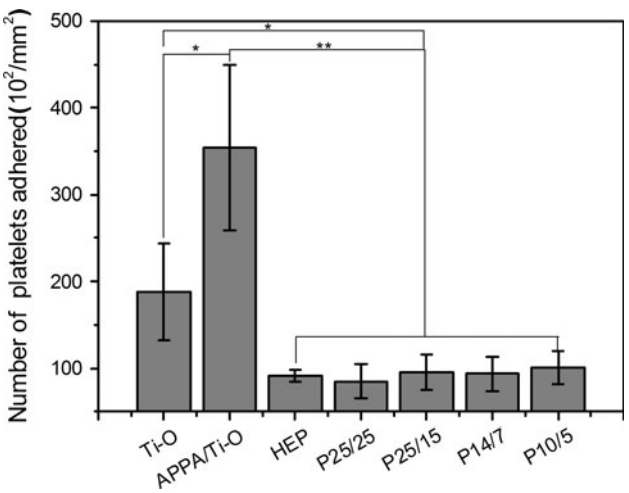

Fig. 9 Number of platelets adhered on the sample surfaces after incubation for 2 h at 37 °C. (*$p < 0.01$, **$p < 0.001$; mean ± SD, $N > 4$)

activate surrounding platelets, and result in thrombus formation [45]. Therefore, the platelet adhesion test is performed to identify the surface thrombogenicity of the samples and to examine the interaction between blood and materials [46]. Figure 8 shows the SEM micrographs of platelets on the different surfaces, and the statistical results of platelets adhered on the surfaces are shown in Fig. 9. The number of adhered platelets on HEP and heparin patterns decreased distinctly compared with APPA/Ti–O and Ti–O. Moreover, the adherent platelets on heparin patterns were almost as many as those on HEP. It has been suggested that the heparin patterns represent the similar efficiency of reducing the platelets adhesion as HEP, although APPA surface enhances platelets adhesion.

The morphology of platelet adhering on the surfaces is also one of the characteristics of biocompatibility, and activation degree of platelets can be related to the changes in their morphology [47]. It is clearly observed that about 25% of the platelets were protruding the sprouts of pseudopod on Ti–O (Fig. 8a). Approximately 28% of the platelets on the APPA/Ti–O extended pseudopods, and 5% were in fully spreading state which indicated the activation of the platelets (Fig. 8b). In comparison, approximately 80% of the platelets adhered to the surface of HEP kept their original spherical shape, indicating an inactivated state (Fig. 8c). Among the heparin patterns (Fig. 8d–g), 60–80% of platelets adhered on APPA covered stripes and their morphologies were similar to those on APPA/Ti–O, and the rest localized on heparin immobilized stripes with the similar activation degree as those on HEP. These results indicate the strong influence on platelet adhesion caused by chemical composition of the surfaces.

Low platelet adhesion and activation expresses good blood compatibility, while a higher degree of platelet adhesion and activation could result in a thrombus. From the adhesion and activation of the adherent platelets, we can conclude that the poor blood compatibility of APPA/Ti–O could be drastically improved by heparin immobilization. It has been suggested that the behavior of platelet adhesion on materials depends strongly on the surface characteristics such as wettability, hydrophilicity/hydrophobicity balance, charge density, etc. [48]. Therefore, the different blood compatibility of materials may be due to their different surface properties. Hydrophilicity is an important factor for evaluation of interactions between biomaterial and cell. Exceptions exist, but generally, the hydrophilic surfaces are more likely to decrease the

adhesion of platelets [49]. However, there are also other factors such as surface charge [50] and functional molecules [5] should be considered. Because the rim of each platelet has a strong negative charge, the material surface with positive charge will induce platelet agglutination [51]. APPA covered surface exhibits a high affinity to platelets, which may attribute to the positive charge due to the amine group of APPA. The heparin-coated surfaces display inhibition of platelet adhesion, which has been proved by previous studies [3, 8, 52]. The reduction of platelet adhesion on heparin patterns mostly attributed to the introduction of heparin. The reduction of platelet adhesion on heparin immobilized surface may attribute to the negatively charge of SO_3^- contained in heparin molecules. However, generally, the anticoagulant activity of surface-bound heparin is believed to depend largely on binding to antithrombin III and subsequent inactivation of coagulation factors such as FIIa, FXa, and FIXa [53]. In addition, the amount of C3 and fibrinogen absorbed on surface plays an important role in mediating platelet adhesion [4]. Therefore, lower adsorption of C3 and fibrinogen on heparin-coated surface than that on non-coated heparin surface may be responsible for the reduction of platelet deposition.

Cell culture

The adhesion and proliferation of endothelial cells were quantitatively evaluated by CCK-8 assay. The results are shown in Fig. 10. The endothelial cells incubated for 1 and 3 days proliferated on all samples except HEP. On the contrary, the number of cells cultured on HEP decreased with increasing incubation time. Among all the samples, APPA/Ti–O induced the fastest proliferation in the culture of 3 days. The number of cells on the patterned samples

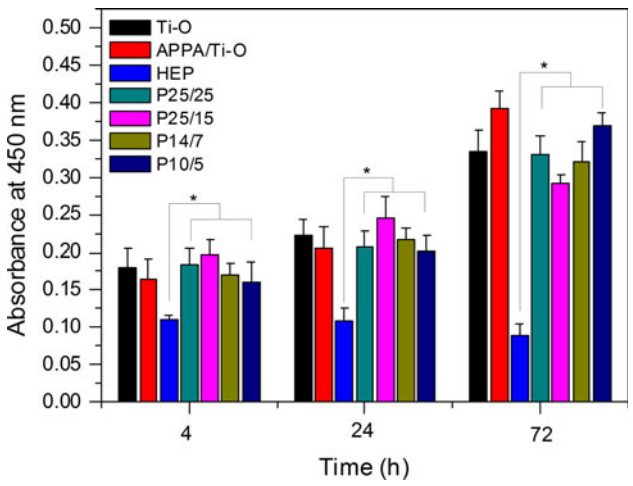

Fig. 10 Proliferation of endothelial cells on sample surfaces after incubation for 4 h, 1 day, and 3 days. Data are presented as mean ± SD of three different experiments, $^*p < 0.01$

was larger than that on HEP at any time. The patterned sample with the smallest pattern size (P10/5) represented almost the same effect on cell proliferation as APPA/Ti–O although heparin stripes were suggested here to inhibit endothelial cell adhesion and growth. The cells on P25/15 demonstrated limited proliferation after incubation for 3 days although their adhesion was the highest in initial 4 h's culture.

The optical micrographs of endothelial cells cultured on different sample surfaces incubated for 4 h, 1 day, and 3 days are shown in Fig. 11. The cells on APPA/Ti–O surface maintained their stretched and cobblestone-like morphology typical of endothelial cells, indicating the good affinity of APPA/Ti–O toward cells. Remarkably, behavior of the cells cultured on the HEP surface was quite opposite to that on APPA/Ti–O, low adhesion, shrinking shape and invisible proliferation, revealing the effect of inhibiting endothelial cell adhesion and growth caused by immobilization of heparin. However, patterned heparin samples demonstrated the effect of high adhesion, good morphology and obvious proliferation, compared to non-patterned heparin sample. Apparently, cell alignment could be found on P25/25 and P25/15 surfaces after 1 and 3 days, and the number of cells on P10/5 was larger than that on other patterned samples at the third day.

The spreading of cells occurred in the early period, which plays a key role in the cells growth [54]. So the average spreading area of the cells incubated for 4 h and 1 day was calculated and further elucidation was made by the statistical analysis (Table 3). The average area of cells incubated for 1 day was much larger than that cultured for 4 h. The smallest spreading area was observed on HEP at these two time points. The spreading area of the cells incubated for 4 h on APPA/Ti–O and patterned samples displayed no significant difference, but much larger than that on Ti–O. After 1 day of incubation, the cells on patterned samples demonstrated much larger spreading area than those on Ti–O. The average area of cells on larger size patterns (P25/25, P25/15, and P14/7) was not significantly different from that on APPA/Ti–O, but the cells on small size pattern (P10/5) were much larger than those on APPA/Ti–O. The larger spreading area of cells on patterned samples may attribute to the influence of the chemical difference and micropattern size.

The statistics of cell morphology including cell length, breadth, L/B, and cellular orientation angle α after 3 days of culture are listed in Table 4. Especially, cells on HEP exhibited the smallest length and breadth among all the samples. The length of the cells on P25/25 and P25/15 was not significantly different from that on APPA/Ti–O and Ti–O, but was much longer than that on P14/7 and P10/5. The breadth of cells on P25/15 was narrower than that on APPA/Ti–O and Ti–O. Length/Breadth (L/B) was used to

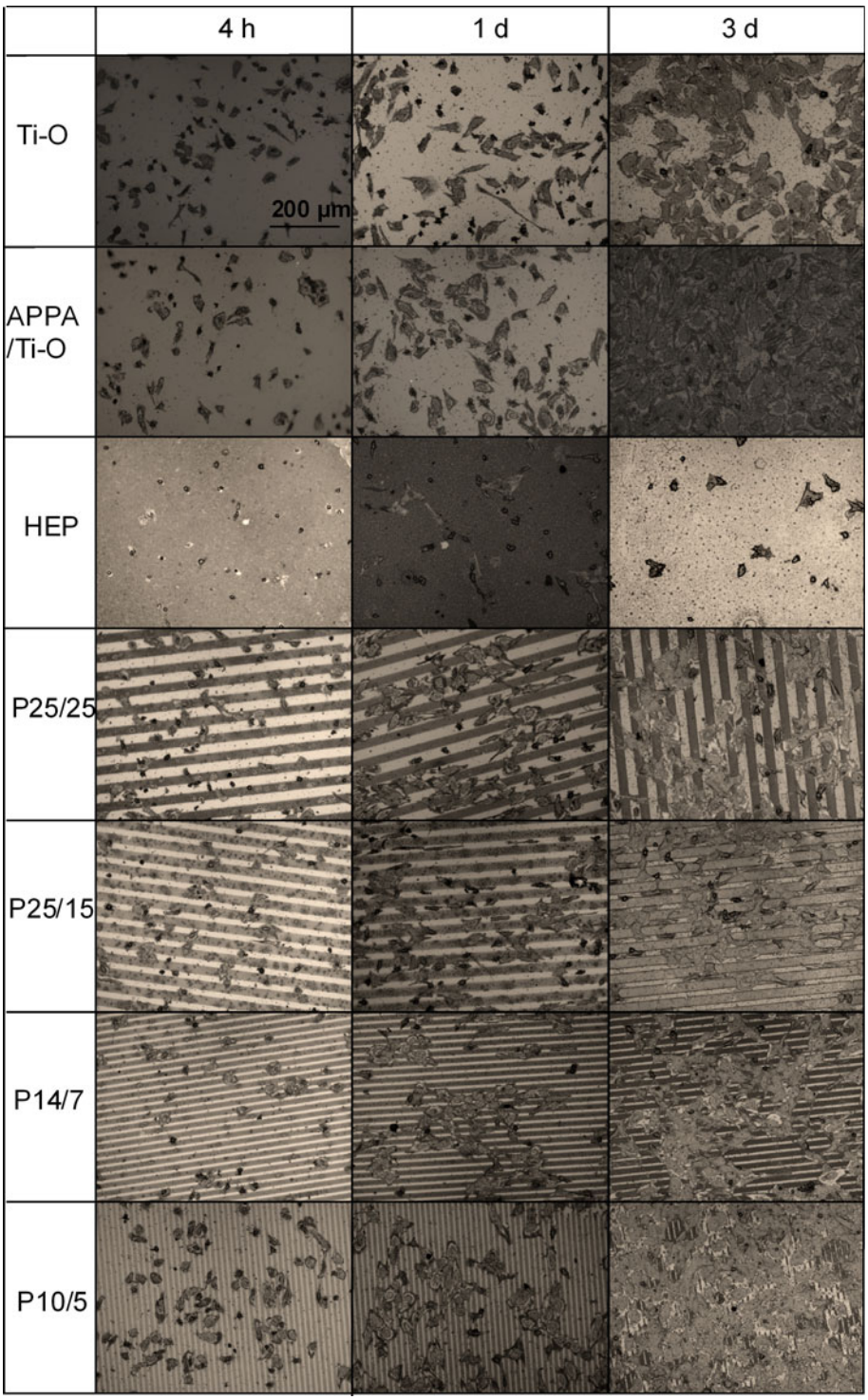

Fig. 11 Morphology of endothelial cells after culturing for 4 h, 1 day, and 3 days, respectively

measure the cell elongation. The cells on P25/15 elongated and aligned along the stripe direction which can be demonstrated from the largest L/B, the smallest orientation angle and the largest proportion of cells aligned within 10° in the direction of the stripes (Table 4). With relatively larger orientation angle and smaller proportion of cells aligned within 10°, cells on P14/7 and P10/5 demonstrated random orientation. It can be suggested that cell shape was affected by the width of stripes.

Some studies indicate that surface properties, such as chemical composition, surface charge, free energy, hydrophilicity, and crystallinity, play roles in cells adhesion and proliferation [55, 56]. Usually, a hydrophilic or positively charged surface is considered to enhance the cell

Table 3 Average area of adherent cells cultured for 4 h and 1 day

Sample	Cell average area (μm^2)	
	Mean ± SD	
	4 h	1 day
Ti–O	611.47 ± 335.00#	1040.23 ± 720.16#
APPA/Ti–O	859.02 ± 289.53*	1306.72 ± 581.59*
HEP	252.85 ± 134.35*#	455.10 ± 328.76*#
P25/25	796.72 ± 238.27*	1428.92 ± 541.91*
P25/15	781.56 ± 268.35*	1325.05 ± 542.86*
P14/7	800.20 ± 285.08*	1403.25 ± 479.28*
P10/5	800.52 ± 372.03*	1544.20 ± 661.78*#

* $p < 0.01$ compared to Ti–O control and # $p < 0.01$ compared to APPA/Ti–O control

compatibility [57, 58]. Therefore, cells spreading and proliferation could be promoted on APPA/Ti–O, which may be attributed to the increase of hydrophilicity and the positive charge carried by its amine groups in aqueous environment [59, 60]. It is debatable about whether heparin inhibits endothelial cell proliferation [61, 62]. Khorana [63] reported that the inhibition of endothelial cell proliferation by heparin depended on molecular weight, and unfractionated heparin (a heterogeneous mixture of polysaccharide molecules with a mean M_r between 12 and 15 kDa) inhibited endothelial cell proliferation. The heparin with a mean M_r of 15 kDa was used in this experiment, so the inhibition effect on endothelial cell proliferation may attribute to the molecular weight. But the interaction mechanism requires a further and deeper investigation. Moreover, the slight increase of hydrophobicity caused by photo-immobilization of AzHep and the conformation change of heparin upon UV irradiation may be another two reasons. The azido group of AzHep could also insert to C–H bond of AzHep upon UV irradiation [33], which may change the conformation of heparin and effect the interactions between heparin and cells.

It is believed that cell shape can govern either individual cell growth or death, and the increased cell spreading leads to cell survival and growth [64]. When cells are round, apoptosis rates are high while growth rates remain insignificant. Conversely, when cells are allowed to spread and flatten to their maximal amount, apoptosis is virtually undetectable while growth rates are high [54]. Therefore, cells on HEP suggested apoptosis due to the round shape and decreased growth rate, while cells on patterned samples showed obvious proliferation which may be attributed to the larger spreading area. Correspondingly, with the largest spreading area, cells on P10/5 exhibited a higher proliferation compared to other patterned samples on the third day.

Cells adhesion and growth can be influenced by the surface topography and chemistry [65]. Topography including height, width, and shape can be sensed as a barrier to the movement of cells. Chemical difference can also be considered to be a barrier where it may allow or prevent cell attachment [66]. It was demonstrated that depth was the most important parameter influencing cellular alignment on grooved patterns [67]. Cell alignment and elongation increased with groove depth [68]. Biela et al. [69] studied the sensitivity of human endothelial cells to topography in the nano–micro range, and found that the minimum groove depth to induce an orientation response and change cell shape was about 100 nm for endothelial cells. Because the height of heparin stripes is about 30 nm, the influence from topography can be excluded, and it is believed that only chemical differences between the microdomains can influence endothelial cell shape and behavior in terms of adhesion, proliferation, and orientation.

Conclusions

Heparin micropatterns on APPA modified Ti–O surface with four different sizes have been prepared and their

Table 4 Statistics of cell morphology (cell length, breadth, L/B, and cellular orientation angle α) incubated for 3 days

Sample	Length (μm)	Breadth (μm)	Length/breadth (L/B)	Average cellular orientation angle α (°)	The proportion of cells with α < 10° (%)
Ti–O	74.3 ± 18.8	38.7 ± 10.9*	2.03 ± 0.66*	/	/
APPA/Ti–O	80.1 ± 15.8	36.4 ± 9.5*	2.37 ± 0.87*	/	/
HEP	20.9 ± 6.8*,#	15.3 ± 4.7*,#	1.43 ± 0.52*,#	/	/
P25/25	74 ± 23	31 ± 8.4*,#	2.46 ± 0.73*	16.35 ± 12.15*	39.81
P25/15	75.5 ± 28	25 ± 9.6#	3.37 ± 1.92#	8.81 ± 8.60	72.83
P14/7	45.5 ± 17.6*,#	26 ± 13.3#	2.00 ± 1.11*,#	20.55 ± 9.25*	13.15
P10/5	50.1 ± 12.7*,#	38.9 ± 8.6*	1.35 ± 0.45*,#	27.61 ± 11.09*	12.50

* $p < 0.01$ compared to P25/15 control and # $p < 0.01$ compared to APPA/Ti–O control

influence on platelets adhesion and endothelial cells behavior was investigated. It is clear that the patterned heparin samples can reduce the platelet adhesion, overcome the inhibition effect on endothelial cell adhesion, spreading, and growth caused by the immobilized heparin and promote the cell spreading and proliferation. Especially, the cells on P25/15 can be regulated by the stripes, elongated, and aligned along the stripe direction, and the cells on P10/5 exhibited much faster proliferation rate than other patterned samples. Therefore, heparin pattern can offer a new method to balance the interaction of endothelial cells with APPA and heparin covered areas and harmonize the functions of both anticoagulation and accelerating endothelialization simultaneously.

Acknowledgement This study was jointly supported by Key basic research program of China (no. 2011CB606204), Natural Science Foundation of China (no. 30870629), and NSFC-RGC Joint Research Funding (30831160509).

References

1. Yang ZL, Wang J, Luo RF, Maitz MF, Jing FJ, Sun H, Huang N (2010) Biomaterials 31:2072
2. Machovich R (1988) Blood vessel wall and thrombosis. CRC Press Inc., Boca Raton
3. Belle EV, Tio FO, Couffinhal T, Maillard L, Passeri J, Isner JM (1997) Circulation 95:438
4. Weber N, Wendel HP, Ziemer G (2002) Biomaterials 23:429
5. Yamazoe H, Oyane A, Nashima T, Ito A (2010) Mater Sci Eng C 30:812
6. Liu TY, Lin WC, Huang LY (2005) Biomaterials 26:1437
7. Kottke-Marchant K, Anderson JM, Umemura Y, Marchant RE (1989) Biomaterials 10:147
8. Aksoy EA, Hasirci V, Hasirci N (2008) J Bioact Compat Polym 23:505
9. Weng YJ, Qi F, Huang N, Wang J, Cheng JY, Leng YX (2008) Appl Sur Sci 255:489
10. Letourneur D, Machy D, Pellé A, Marcon-Bachari E, D'Angelo G, Vogel M, Chaubet F, Michel JB (2002) J Biomed Mater Res 60:94
11. Murray RD, Deitcher SR, Shah A, Jasper SE, Bashir M, Grimm RA, Klein AL (2001) J Am Soc Echocardiogr 14:200
12. Ingber DE (1990) Proc Natl Acad Sci USA 87:3579
13. Beumer S, Ijsseldijk MJ, Degroot PG, Sixma JJ (1994) Blood 84:3724
14. Ni HY, Papalia JM, Degen JL, Wagner DD (2003) Blood 102:3609
15. Falconnet D, Csucs G, Michelle Grandin H, Textor M (2006) Biomaterials 27:3044
16. Petersen SB, di Gennaro AK, Neves-Petersen MT, Skovsen E, Parracino A (2010) Appl Opt 49:5344
17. Parracino A, Gajula GP, di Gennaro AK, Correia M, Neves-Petersen MT, Rafaelsen J, Petersen SB (2011) Biotechnol Bioeng 108:999
18. Parracino A, Neves-Petersen MT, di Gennaro AK, Pettersson K, Lövgren T, Petersen SB (2010) Protein Sci 19:1751
19. Ito Y (1999) Biomaterials 20:2333
20. Ostuni E, Chen CS, Ingber DE, Whitesides GM (2001) Langmuir 17:2828
21. Aubin H, Nichol JW, Hutson CB, Bae H, Sieminski AL, Cropek DM, Akhyari P, Khademhosseini A (2010) Biomaterials 31:6941
22. Hwang CM, Park Y, Park JY, Lee K, Sun K, Khademhosseini A, Lee SH (2009) Biomed Microdevices 11:739
23. Carrell R, Skinner R, Wardell M, Whisstock J (1995) Mol Med Today 1:226
24. Ragosta M, Karve M, Brezynski D (1999) Am Heart J 137:250
25. Krupinski K, Basic-Micic M, Lindhoff E, Breddin HK (1990) Blut 61:289
26. Michanetzis GPA, Katsala N, Missirlis YF (2003) Biomaterials 24:677
27. Tsyganov I, Maitz MF, Wieser E (2004) Appl Sur Sci 235:156
28. Gawalt ES, Avaltroni MJ, Koch N, Schwartz J (2001) Langmuir 17:5736
29. Ni YX, Feng B, Wang JX, Lu X, Qu SX, Weng J (2009) J Mater Sci 44:4031. doi:10.1007/s10853-009-3562-0
30. Lee JH, Jung HW, Kang IK, Lee HB (1994) Biomaterials 15:705
31. Harsch A, Calderon J, Timmons RB, Gross GW (2000) J Neurosci Methods 98:135
32. Konno T, Hasuda H, Ishihara K, Ito Y (2005) Biomaterials 26:1381
33. Bora U, Sharma P, Kannan K, Nahar P (2006) J Biotechnol 126:220
34. Hinrichs WLJ, ten Hoopen HWM, Wissink MJB, Engbers GHM, Feijen J (1997) J Control Release 45:163
35. Ding MH, Wang BL, Li L, Zheng YF (2010) Surf Coat Technol 204:2519
36. Xu M, Qiu J, Lin Y, Shi X, Chen H, Xiao T (2010) Colloids Surf B 80:200
37. Chen JY, Wan GJ, Leng YX, Yang P, Sun H, Wang J, Huang N (2004) Surf Coat Technol 186:270
38. Dai ZW, Zou XH, Chen GQ (2009) Biomaterials 30:3075
39. den Braber ET, de Ruijter JE, Smits HTJ, Ginsel LA, von Recum AF, Jansen JA (1996) Biomaterials 17:1093
40. Yang SP, Lee TM (2011) J Mater Sci Mater Med. doi: 10.1007/s10856-011-4255-1
41. Park YS, Ito Y (2000) Cytotechnology 33:117
42. Siqueira Petri DF, Wenz G, Schunk P, Schimmel T (1999) Langmuir 15:4520
43. Quiñones R, Gawalt ES (2007) Langmuir 23:10123
44. Huang XJ, Guduru D, Xu ZK, Vienken J, Groth T (2011) Macromol Biosci 11:131
45. Milner KR, Snyder AJ, Siedlecki CA (2006) J Biomed Mater Res A 76:561
46. Chen JL, Li QL, Chen JY, Chen C, Huang N (2009) Appl Surf Sci 255:6894
47. Ko TM, Lin JC, Cooper SL (1993) Biomaterials 14:657
48. Park JB (1984) Biomaterials science and engineering. Plenum Press, New York
49. Rodrigues SN, Gonçalves IC, Martins MCL, Barbosa MA, Ratner BD (2006) Biomaterials 27:5357
50. Sharma CP (1994) Bull Mater Sci 7:1317
51. Sagnella S, Mai-Ngam K (2005) Colloids Surf B 42:147
52. Huang XJ, Erdtmann M, Keller R, Baumann H (1994) Biomaterials 15:1043
53. Sanchez J, Elgue G, Riesenfeld J, Olsson P (1995) J Biomed Mater Res 29:655
54. Chen CS, Mrksich M, Huang S, Whitesides GM, Ingber DE (1998) Biotechnol Prog 14:356
55. Qu XH, Wu Q, Chen GQ (2006) J Biomater Sci Polymer Edn 17:1107
56. Qiu Q, Sayer M, Kawaja M, Shen X, Davies JE (1998) J Biomed Mater Res 42:117
57. García AJ, Boettiger D (1999) Biomaterials 20:2427
58. Lee JH, Lee JW, Khang G, Lee HB (1997) Biomaterials 18:351

59. Sanborn SL, Murugesan G, Marchant RE, Kottke-Marchant K (2002) Biomaterials 23:1
60. Wan YQ, Yang J, Yang JL, Bei JZ, Wang SG (2003) Biomaterials 24:3757
61. Wissink MJB, Beernink R, Pieper JS, Poot AA, Engber GHM, Beugeling T, van Aken WG, Feijen J (2001) Biomaterials 22:151
62. Meng S, Liu ZJ, Shen L, Guo Z, Chou LL, Zhong W, Du QG, Ge JB (2009) Biomaterials 30:2276
63. Khorana AA, Sahni A, Altland OD, Francis CW (2003) Arterioscler Thromb Vasc Biol 23:2110
64. Chen CS, Mrksich M, Huang S, Whitesides GM, Ingber DE (1997) Science 276:1345
65. Magnani A, Priamo A, Pasqui D, Barbucci R (2003) Mater Sci Eng C 23:315
66. Anselme K, Davidson P, Popa AM, Giazzon M, Liley M, Ploux L (2010) Acta Biomater 6:3824
67. Loesberg WA, te RJ, van Delft FC, Schon P, Figdor CG, Speller S, van Loon JJ, Walboomers XF, Jansen JA (2007) Biomaterials 28:3944
68. Andersson AS, Olsson P, Lidberg U, Sutherland D (2003) Exp Cell Res 288:177
69. Biela SA, Su Y, Spatz JP, Kemkemer R (2009) Acta Biomater 5:2460